

## MORPHOLOGY AND PATHOMORPHOLOGY

# Ultrastructure of Blood and Lymph Bronchial Capillaries in Inflammation and Endobronchial Laser Therapy

V. V. Polosukhin

Translated from *Byulleten' Eksperimental'noi Biologii i Meditsiny*, Vol. 123, No. 2, pp. 222-228, February, 1997  
Original article submitted December 22, 1995

Structural alterations occurring in blood and lymph microcapillaries during inflammation of the mucous membrane of large bronchi and morphogenic effects of endobronchial laser therapy are described. The data are interpreted in terms of epitheliostromal correlations.

**Key Words:** *bronchial inflammation; bronchial biopsy; blood and lymph capillaries; laser therapy*

Low-energy laser radiation has found wide application in pulmonology [2,3,6-8]. However, the morphology of regenerative processes induced by laser light is poorly investigated. In the present study we examined ultrastructural modifications occurring in blood and lymph capillaries of large bronchi during inflammation and the effect of laser radiation on them.

### MATERIALS AND METHODS

A total of 188 bioptates of lobular and segmental bronchi from 76 patients with acute, gangrenous, and chronic abscesses, chronic pneumonia, and tuberculosis were studied. Sixty-three patients (162 bioptates) received both conventional and endobronchial laser therapy. Laser irradiation was performed during bronchoendoscopy: scattered light from an LG-75 laser ( $\lambda=632.8$  nm, 3 mW) was applied. The number of sessions was determined by therapeutic effectiveness (2-6 sessions lasting 3-5-min). Bronchial biopsy was performed before each session. Control bioptates from 13 patients on conventional therapy were obtained before and after treatment.

Some tissue specimens (1 mm<sup>3</sup>) were incubated in medium 199 containing <sup>3</sup>H-uridine or <sup>3</sup>H-thymidine and analyzed by radioautography. Radioautographs of semithin sections (5-day exposure) were prepared by the method [9]. Other tissue specimens were fixed in 4% paraformaldehyde and 1% osmium tetroxide and embedded in Epon-Araldite. Paraffin, semithin, and ultrathin sections were prepared from each bioptate.

### RESULTS

According to the classification of ultrastructural changes in the epithelium of large bronchi in chronic lung inflammation [5], the bioptates were divided into four groups.

In group 1 bioptates, blood and lymph capillaries with physiological plethora predominated. The stratified columnar structure of the epithelium and ciliated cells were preserved.

In groups 2 and 3, a higher degree of blood capillary plethora and focal infiltration by lymphocytes and plasmacytes were observed. Endothelial cells were hypertrophied (Fig. 1, *a*) and actively incorporated <sup>3</sup>H-uridine (Table 1). Most lymph capillaries were dilated and plethoric (Fig. 1, *b*), the

Institute of Experimental and Clinical Lymphology, Siberian Division of the Russian Academy of Medical Sciences, Novosibirsk

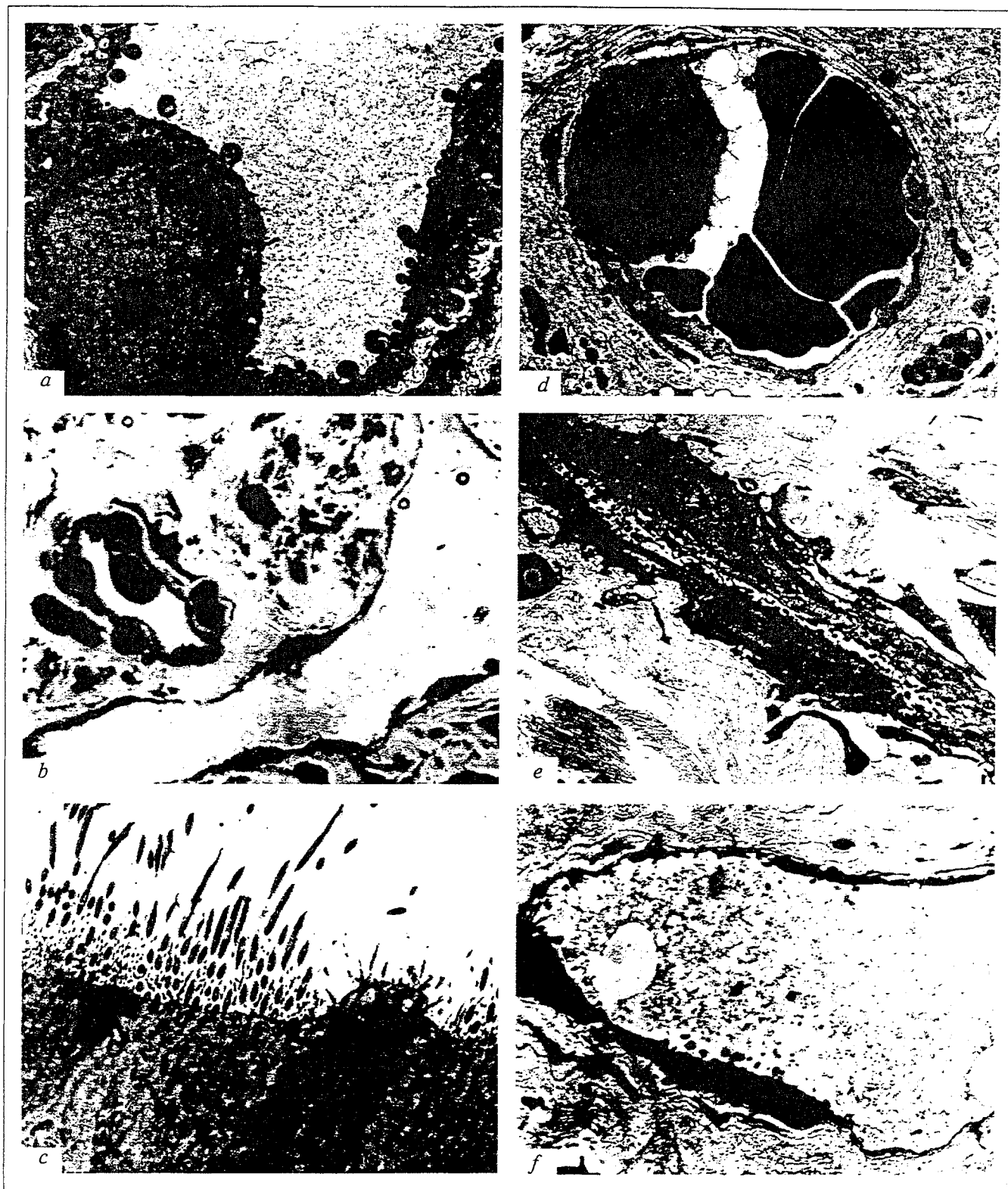


Fig. 1. Ultrastructure of bronchial mucosa in acute and chronic lung diseases.

- a) hypertrophy of endothelial blood capillary, magnification 3300;
- b) lymph capillary lumen. Semithin section, azure II staining; magnification 600;
- c) alteration of ciliated epitheliocytes and degeneration of goblet glandulocytes, magnification 3300;
- d) thin endothelial lining in blood capillary, magnification 2600;
- e) obliteration of a venule; hypertrophy of collagen fibers in the perivascular zone; magnification 2000;
- f) thin endothelial lining of lymph capillary, magnification 3300.

**TABLE 1.** Radioautographic Analysis of RNA and DNA Syntheses in Bronchial Epithelium and Endotheliocytes of Blood Capillaries of Bronchial Mucosa During Inflammation and Endobronchial Laser Therapy ( $M \pm m$ )

Bioplate	Label index before and after irradiation		
	before	after 6-8 days	>20 days
<b>Bronchial epitheliocytes</b>			
group 1 ( $n=3$ )	60.3±4.8/1.38±0.08		
groups 2 and 3 ( $n=8$ )	68.3±4.2/2.34±0.59*	73.2±5.2/3.84±0.48**	
group 4 metaplasia ( $n=5$ )	38.5±4.0*/8.41±0.87*	72.9±5.6**/3.98±0.24**	90.8±4.4**/2.78±0.73
group 4 atrophy ( $n=4$ )	33.9±6.6*/0.92±0.08*	77.3±6.0**/3.58±0.32**	
<b>Blood capillary endotheliocytes</b>			
group 1 ( $n=3$ )	61.3±3.7/—		
groups 2 and 3 ( $n=8$ )	78.6±2.5*/—	98.5±0.4**/—	
group 4 metaplasia ( $n=5$ )	46.9±4.4*/—	98.3±0.3**/—	99.8±0.1**/—
group 4 atrophy ( $n=4$ )	36.9±2.6*/—	97.9±0.4**/—	

**Note.** Numerator is the label index after incubation with  $^3\text{H}$ -uridine. Denominator is the label index after incubation with  $^3\text{H}$ -thymidine.  $p < 0.05$ : \*compared with group 1; \*\*compared with the corresponding value before irradiation.

degree of these alterations was consistent with the intensity of hyperemia and edema.

In group 2 bioplates, alterations of epitheliocytes and hyperplasia of glandulocytes were observed, while in group 3, epitheliocytic alterations coincided with degeneration of glandulocytes (Fig. 1, c).

Enhanced function of blood capillaries and intensification of metabolic processes in endothelial cells were accompanied by an increase in proliferative and metabolic activities of bronchial epitheliocytes in comparison with those observed in group 1 (Table 1). Therefore, we decided to pool the radioautographic data for the bioplates of groups 2 and 3.

Changes in the epitheliocyte differentiation were observed in group 4 bioplates. The occurrence of metaplasia of stratified squamous epithelium was higher than that of atrophy with formation of mono- or bilayer epithelium. Changes in differentiation coincided with a decrease in metabolic activity and variations in proliferative activity of epithelial cells (Table 1).

Atrophy or sclerosis in combination with polymorphous-cellular infiltration against the background of reduced blood flow were typical changes occurring in the lamina propria of group 4 bioplates. Sclerosis was most pronounced in the perivascular zone and subendothelial basement membrane. In the majority of capillaries, the endothelium thickness decreased (Fig. 1, d), and the nuclei protruded into the lumen. The number of pinocytic vesicles decreased considerably. The majority of postcapillary venules were collapsed, although the ultrastructure of their epitheliocytes — numerous invaginations of the nuclear membrane, accumulation of organelles in the perinuclear zone, and numerous cytoplasmic processes

on the basal and luminal surfaces (Fig. 1, e) — indicated an increase in functional activity. The state of lymph capillaries was typical of lymph stasis. Most highly plethoric capillaries with thin walls looked like cavities filled with lymph (Fig. 1, f).

On days 6-8 after laser irradiation, pronounced hyperplasia of basal cells without differentiation to typical cell elements was observed. This was regarded as a transitory state (pseudometaplasia) [8].

The lamina propria was characterized by pronounced hyperemia (Fig. 2, a) and leukostasis (Fig. 2, b) with neutrophil and lymphocyte migration into the perivascular tissue (Fig. 2, c). The ultrastructure of blood capillaries reflected increased functional load on these cells. These changes were often followed by proliferation of blood capillaries with focal formation of the granulation tissue. The structure and function of lymph capillaries were restored (Fig. 2, d).

Radioautography revealed an increase in metabolic activity of epithelial, endothelial, and stromal cells. In all bioplates, almost 100% of endotheliocytes in blood (Fig. 2, e) and lymph (Fig. 2, f) capillaries incorporated  $^3\text{H}$ -uridine. The intensity of proliferative activity varied (Table 1). Some endothelial cells and pericytes also incorporated  $^3\text{H}$ -thymidine.

These changes persisted for various time periods. Generally, the degree of hyperemia, leukodiapedesis, and cell infiltration decreased one month after laser irradiation. Then blood vessels with cuboidal endothelium resembling the lymphoid tissue venules (Fig. 3, a) appeared against the background of preserved diapedesis of neutrophil leukocytes. This was accompanied by an increase in the number of lymphocytes and plasma cells in the infiltrate as a result of their diapedesis from these vessels [13,15]. Numerous

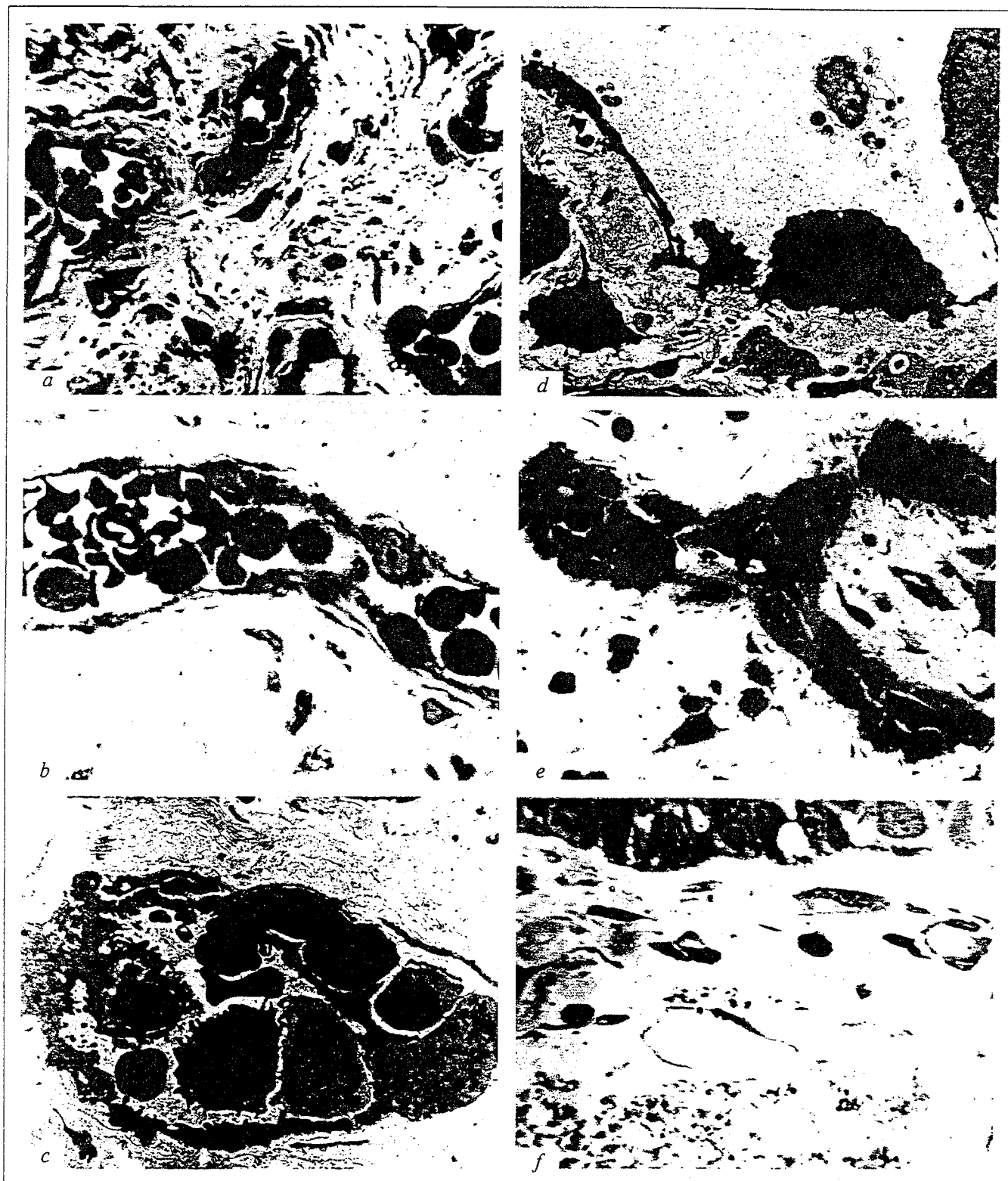


Fig. 2. Ultrastructure of bronchial mucosa after endobronchial laser therapy of acute and chronic inflammatory lung diseases (early stage).

- a) plethora of blood capillaries, magnification 600;  
 b) plethora and leukostasis in blood capillary, magnification 1000;  
 c) migration of neutrophil leukocytes into the stroma, magnification 2600;  
 d) lymph capillary of the mucous membrane; magnification 2600;  
 e) intense synthesis of RNA in blood capillary endotheliocytes, magnification 1000;  
 f) RNA synthesis in lymph capillary endotheliocytes, magnification 600.  
 a, b, e, f) semithin sections, staining with azure II; e, f) incubation with  $^3\text{H}$ -uridine.

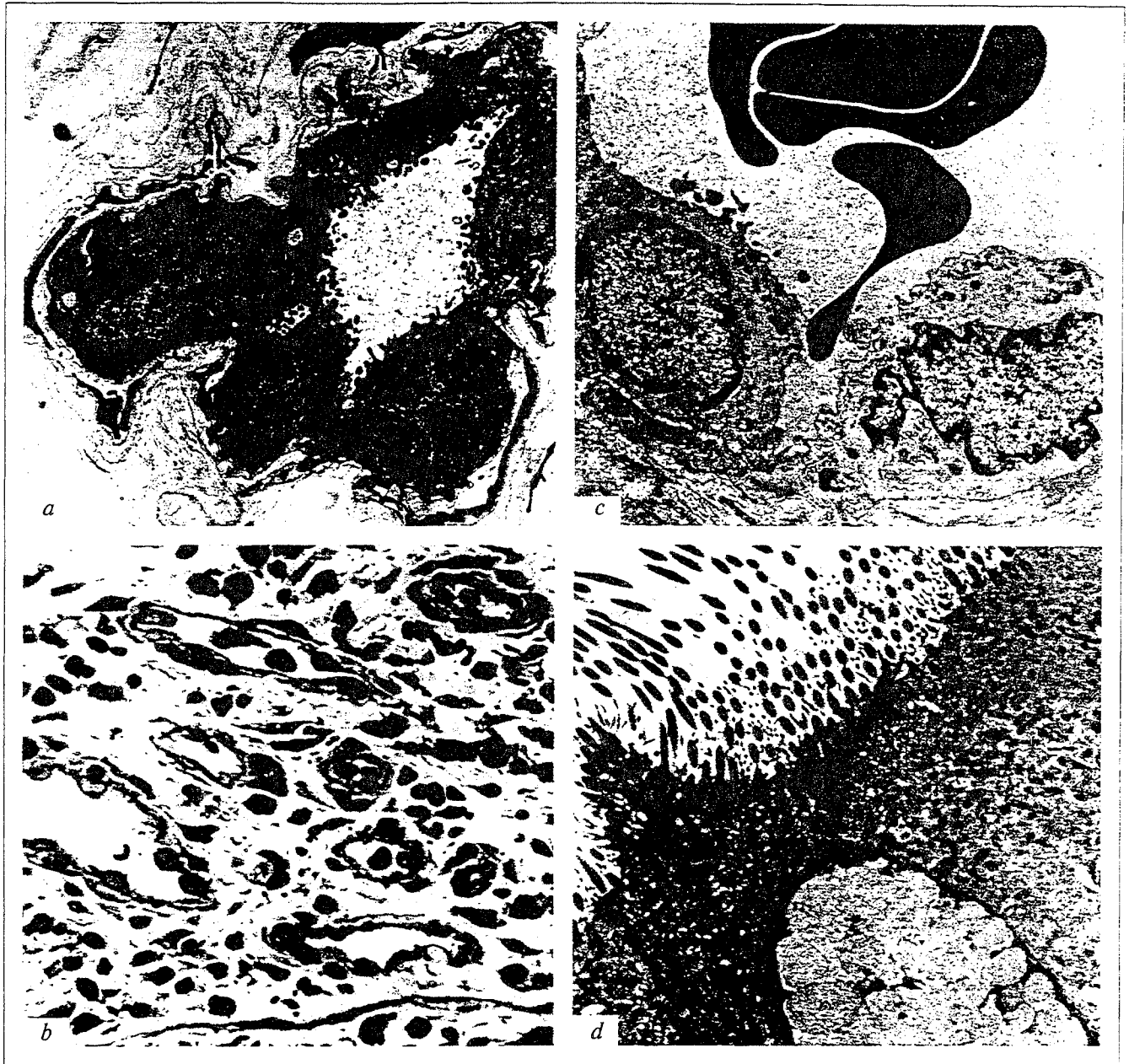


Fig. 3. Ultrastructure of bronchial mucosa after endobronchial laser therapy of acute and chronic inflammatory lung diseases (remote results). a) postcapillary venule of cuboidal endothelium, magnification 2600; b) *de novo* synthesized connective tissue with numerous capillaries and fine collagen fibers. Semithin section, staining with azure II, magnification 600; c) blood capillary endotheliocytes with structural signs of increased functional activity, magnification 3300; d) restored structure of bronchial epithelium, magnification 3300.

fibroblasts with the ultrastructure typical of intense protein production were observed in the lamina propria. Then fine collagen bundles gradually replaced the foci of granulation tissue and inflammation infiltrates. The *de novo* synthesized collagen had a higher content of extracellular matrix and thin regularly oriented collagen bundles (Fig. 3, b). The structure of blood capillaries reflected the increase in their functional activity (Fig. 3, c).

Transformation of the surface bronchial epithelium coincided with decline in the inflammatory

processes. Pronounced hyperplasia of epithelial cells was followed by formation of transitional epithelium, which was replaced by stratified ciliated epithelium (Fig. 3, d).

Structural changes caused by laser radiation varied in intensity and terms depending on the nature of pathological process, degree of inflammatory reaction in the bronchi, and the number of irradiation sessions.

The above-mentioned changes were not observed in patients receiving conventional therapy. The following processes occurred in their bronchi: reduction

in the epitheliocytic modifications, mucous hyperemia, and edema.

Acceleration of cell renewal and increased metabolism of bronchiocytes in group 2 and 3 bioplates compensated for cell deficiency due to cell damage and death. However, chronic "irritation" of bronchial mucosa is accompanied by progressing insufficiency of lymph and then blood system. This leads to tissue hypoxia triggering atrophic and sclerotic processes in the mucosa. As a result, the intensity of metabolic reactions in endotheliocytes and pericapillary cells (active zone of the stroma) decreased. These tendencies affect the basal-cellular proliferation, changing primarily the microenvironment of basal cells in the surface epithelium, which impairs differentiation of bronchial epithelium.

Hyperplasia of bronchial epithelium with synchronous transformation of the connective tissue and restoration of the mucous membrane to almost normal condition are the specific processes induced by laser radiation. Transformation of blood and lymph vessels reflects their activation. The structure of lymph vessels is rapidly restored, which is accompanied by normalization of the drainage function. Capillary reactions vary in a wide range. Pronounced plethora and leukocyte migration into the stroma with subsequent proliferation of capillaries and focal formation of the granulation tissue are the classical manifestations of intense inflammatory reactions [10]. Restoration of morphological structure following the acute phase of inflammation is a unique phenomenon.

Common and coupled pathogenic mechanisms of pathological processes and morphogenesis of re-

storative processes in induced regenerative reactions can be interpreted in terms of structural and functional unity of lymph and blood systems [1,11].

## REFERENCES

1. Yu. I. Borodin, M. R. Sapin, L. E. Etingen, *et al.*, *General Anatomy of the Lymphatic System* [in Russian], Novosibirsk (1990).
2. E. V. Demicheva, *Sov. Med.*, No. 2, 32-36 (1991).
3. B. V. Klimanskaya, A. B. Shekhter, V. Kh. Sosyura, *et al.*, *Grud. Khir.*, No. 4, 59-64 (1989).
4. A. S. Kryuk, V. A. Mostovnikov, I. V. Khokhlov, and N. S. Serdyuchenko, *Therapeutic Effectiveness of Low-Energy Laser Radiation* [in Russian], Minsk (1986).
5. G. I. Nepomnyashchikh, *Pathological Anatomy and Ultrastructure of Bronchi in Chronic Lung Inflammation* [in Russian], Novosibirsk (1979).
6. L. M. Nepomnyashchikh, V. V. Polosukhin, G. I. Nepomnyashchikh, and V. P. Tumanov, *Byull. Eksp. Biol. Med.*, **104**, No. 12, 743-749 (1987).
7. L. M. Nepomnyashchikh, V. V. Polosukhin, and G. I. Nepomnyashchikh, *Ibid.*, **108**, No. 7, 117-121 (1989).
8. V. V. Polosukhin, S. M. Egunova, and S. G. Chuvakin, *Morphogenetic Effects of Laser Radiation in the Therapy of Acute and Chronic Bronchitis* [in Russian], Novosibirsk (1993).
9. D. S. Sarkisov, A. A. Pal'tsyn, B. V. Vtyurin, *Electron Microscopic Radioautography of the Cell* [in Russian], Moscow (1980).
10. A. I. Strukov and V. V. Serov, *Pathological Anatomy* [in Russian], Moscow (1995).
11. V. A. Shakhlamov and A. M. Tsameryan, *Ultrastructural Organization of Lymph Vessels* [in Russian], Novosibirsk (1982).
12. W. A. Cornelius, *Australas Phys. Eng. Sci. Med.*, **6**, No. 3, 100-105 (1983).
13. A. J. Freemont, *J. Clin. Pathol.*, **36**, No. 2, 161-166 (1983).
14. R. Senz and G. Muller, *Ber. Bunsen-Ges. Phys. Chem.*, **93**, No. 3, 269-277 (1989).
15. H. B. Stamper and J. J. Woodruff, *J. Exp. Med.*, **144**, No. 4, 828-833 (1976).